Theoretical Studies on the Mechanism of C−P Bond Cleavage of a Model α-Aminophosphonate in Acidic Condition†

Marek Doskocz,‡,§ Szczepan Roszak,‡,|| D. Majumdar,‡ Jacek Doskocz,§ Roman Gancarz,§ and Jerzy Leszczynski*,‡

Computational Center for Molecular Structure and Interactions, Jackson State University, Jackson, Mississippi 39217, Department of Medicinal Chemistry and Microbiology, Faculty of Chemistry, and Institute of Physical and Theoretical Chemistry, Wroclaw University of Technology, Wybrzeże Wyspiańskiego 27, 50-370 Wroclaw, Poland

Received: August 3, 2007; In Final Form: August 31, 2007

Various reaction paths of the P−C bond cleavage of α-aminophosphonates in acidic media, resulting in the derivatives of phosphonic acid, has been investigated using density functional level of theories in the gas phase as well as in aqueous medium. Dimethyl (α-anilinobenzyl)phosphonate has been used as the model molecule and our investigation confirms a three steps process including protonation, P−C bond cleavage, and the transformation of the products from the final transition state (imine cation and H-phosphonate) through hydrolysis. The most favorable reaction path starts from the amino group protonation, followed by a proton transfer through N−H···O(P) hydrogen bond, and the P−C bond cleavage from the resulting protonated structure. Explicit inclusion of water molecules indicated that two waters are needed for the P−C bond cleavage, and the calculated mechanistic paths in this hydrated model are similar to those of the aqueous solvation model.

1. Introduction

α-Aminophosphonates are mimetic of natural amino acids.[1−3] In these classes of compounds, the carboxylic group (−COOH) is replaced by phosphonic acid fragment (−P(O)(OH)$_2$). This difference between these two classes of compounds is reflected in their shape (flat carboxylic versus tetrahedral phosphonic group), size (phosphorus atom is significantly larger than carbon), acidity (phosphonic acid is more acidic), and several other properties.[3] These compounds possess interesting biological properties and find applications as haptens (in catalytic antibodies),[3] inhibitors of enzymes such as HIV-proteases,[3,4] renin,[5] EPSP synthase (3-phosphoshikimate-1-carboxyvinyl-transferase (5-enolpyruvylahikimate-3-phoshate-synthase),[6] and neuropeptidase NAALADase (N-acetylated-alpha-linked acidic dipeptidase).[7] Some of the aminophosphonates are also applied in antiviral, antibacterial, or anticancer drugs and in the osteoporosis treatment. In addition, these compounds are of commercial importance as herbicides (e.g. Roundup).[3,8]

The P−C bond cleavage is known to be one of the most important phenomena of such molecules essential in several of their biological tasks. Despite the fact that aminophosphonates are rather stable compounds, their P−C bond cleavage was observed in basic,[9] neutral,[10] and acidic[11] media. These cleavage reactions are also catalyzed by enzymes in living organisms.[12,13] The P−C bond breaking generally leads phosphorus to form derivatives of phosphonic (H_3PO_3) or phosphoric acid (H_3PO_4) in the final products. The factors which control the formation of the products in such cleavage reactions include the structural characteristics of the reactants, path of the reaction followed (mechanism), and the physical conditions applied. Both homolytic[12] and heterolytic mechanisms[9] were postulated for such a cleavage, but the mechanism is still not well-understood.[8] This uncertainty of understanding the mechanism of P−C bond cleavage of α-aminophosphonates warrants detailed theoretical studies on such reactions as not much effort has been made in this direction. The present paper explores the probable mechanistic paths of the P−C bond cleavage (which leads to the formation of derivatives of phosphonic acid) of a model α-aminophosphonate, dimethyl (α-anilinobenzyl)phosphonate (DMABP; Scheme 1), in acidic medium using state of the art quantum chemical techniques.

It was shown that the P−C bond cleavage of diethyl esters of (α-anilinobenzyl)phosphonates takes place in acidic environment.[14,15] Time dependent NMR (nuclear magnetic resonance) studies of these compounds in aqueous acidic media and at a high temperature indicated the presence of diester, monoester, (α-anilinobenzyl)phosphonates, and phosphonic acid (Figure 1s, Supporting Information). The analysis of concentrations of components in solution indicates that at least a large part of phosphonic acid originates from the direct decomposition of diester. Additionally, as indicated by Deron et al.[14] the initiation of the reaction takes place through the protonation of oxygen of the phosphonic group. The amino group of the aniline part is a competitive site for such a protonation, and experimental studies indicated a correlation between the acidity of amino group and the kinetics of the reaction.[14] On the basis of the available experimental evidence, the mechanism of P−C bond decomposition is assumed to proceed through three consecutive steps, namely, protonation of phosphonates, P−C bond cleavage, and conversion of transition products into final derivatives of phosphonic acid. Our present theoretical studies address all of these reaction steps for the decomposition of DMABP into derivatives of phosphonic acid in acidic media through the P−C

† Part of the "William A. Lester, Jr., Festschrift".
* Corresponding author, E-mail: jerzy@ccmsi.us.
‡ Jackson State University.
§ Department of Medicinal Chemistry and Microbiology.
|| Institute of Physical and Theoretical Chemistry.

10.1021/jp0762370 CCC: $40.75
Published on Web 11/15/2007

SCHEME 1: Dimethyl (α-anilinobenzyl)phosphonate (DMABP)

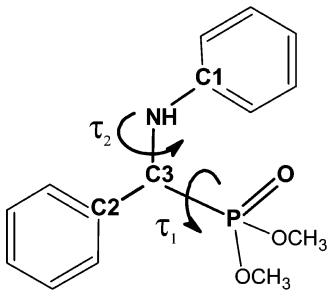

bond cleavage. We have further analyzed the role of hydration on the reaction paths through predictions of the stepwise addition of water molecules to the reactive systems.

2. Theoretical Methods and Computational Details

The structures of the different conformers of DMABP and its protonated forms were optimized using the density functional theory (DFT).[16] The DFT approach applied here utilizes Becke's three parameter functional[17] with the local correlation part of Vosko et al.[18] and the nonlocal part of Lee et al.[19] (abbreviated as B3LYP). No symmetry constraints were imposed during the optimization process. The calculations were performed using the standard 6-31G(d,p) basis set.[20] Additionally, single point calculations, for the selected structures, were carried out in 6-311++G(d,p) basis.[21] The transition state structures involving P−C cleavage of DMPBP were determined by quadratic synchronous transit (QST2) method.[22] The effect of solvent on the calculated structures has been taken into account through the polarized continuum model using the conductor-like screening reaction field (COSMO).[23] Vibrational frequencies and thermodynamic properties of studied complexes were calculated applying the ideal gas, rigid rotor, and harmonic oscillator approximations.[24] The charge distribution was studied applying the Mulliken population analysis. The discussion regarding atomic charges should be treated with caution however because of large differences between different population schemes. The computations were carried out using the Gaussian 03 suite of codes.[25]

3. Results and Discussion

3.1. Conformational Analysis and Proton Affinity of DMABP. The conformational analysis of DMABP was carried out for a number of possible arrangements including the one known from its crystal structure.[26] The differences between the conformers are expressed in terms of two dihedral angles τ_1(N−C3−P−O) and τ_2(C1−N−C3−C2) (Scheme 1). The molecule possesses several low-energy conformers which are characterized by the absence of imaginary vibrational frequencies. They are presented in Table 1. The conformer originating from the crystal structure (M1, Table 1) is one of the low-energy conformers but not the global minimum structure. The energy difference (ΔE) between the conformers M2, M4, and M6 are very low, and all of them could probably coexist in the gas phase. The conformers M3 and M5 are relatively high-energy conformers as estimated from their ΔE values. The $\Delta(E + \mathrm{ZPE})$ and ΔG values in the gas phase follow the same trend. In aqueous medium, this conformational scenario is a bit different. Although the respective conformers maintain the same energy order, the M2 conformer is much more stabilized in aqueous medium with respect to the other conformers.

The two probable protonation sites of DMABP are the nitrogen (of the aniline part) and oxygen (attached to the P atom) atoms. In the case of the nitrogen protonated structures, all of

TABLE 1: P−C Distances (l_{P-C}, Å), Dihedral Angles τ_1(N−C_3−P−O), τ_2(C_1−N−C_3−C_2) (in Degrees) and Energy Differences (kcal/mol) from Energetically Lowest Structure (Electronic Energy, ΔE; Electronic Energy Corrected for Zero Point Energy, $\Delta(E + \mathrm{ZPE})$; Free Enthalpy at 293 K, ΔG; and Free Enthalpy Including Solvent Effects, ΔG_{aq}) of DMABP, Its N-Protonated and O-Protonated Forms, and the Transitin States Involved[a]

complex	l_{P-C}	τ_1	τ_2	ΔE	$\Delta(E + \mathrm{ZPE})$	$\Delta(E + \mathrm{ZPE})^c$	ΔG	ΔG_{aq}
				Conformers of DMABP				
M1	1.854	70.4	−131.2	1.6	1.6	1.4	1.7	0.0
M2	1.846	−65.0	−118.8	0.4	0.2	0.0	−0.4	−1.4
M3	1.855	176.1	−152.1	8.1	7.9	7.6	7.1	5.4
M4[b]	1.864	17.7	−83.3	0.0	0.0	0.0	0.0	0.0
M5	1.850	−74.7	42.6	4.0	4.2	4.4	4.3	2.4
M6	1.850	163.8	−82.4	0.2	0.2	−0.1	0.5	0.1
				Conformers of N-Protonated DMABP				
NH^+1	1.868	78.1	−127.6	3.8	3.8	3.4	3.4	0.9
NH^+2[b]	1.870	−24.5	−143.7	0.0	0.0	0.0	0.0	0.0
NH^+3	1.864	−163.5	−121.5	4.9	4.8	4.2	3.8	−0.8
NH^+4	1.869	26.3	−84.5	0.8	0.6	0.2	0.1	0.3
NH^+5	1.856	−53.3	−60.2	0.9	0.9	0.6	0.4	−0.5
NH^+6	1.862	161.8	−74.8	3.1	3.1	4.5	2.9	−1.7
				Hydrogen Bond Transition State				
$TS(NH^+O)$	1.869	−11.8	−127.0	9.0	5.7	6.5	5.6	10.2
				Conformers of O-Protonated DMABP				
OH^+1	1.850	53.2	−155.5	11.1	8.7	7.5	8.0	13.7
OH^+2	1.867	−19.6	−133.0	7.4	5.9	5.6	6.0	8.2
OH^+3	1.840	173.8	−118.9	11.9	9.7	7.9	9.2	8.8
OH^+4	1.854	23.0	−92.2	9.0	7.2	6.7	6.0	9.5
OH^+5	1.847	26.5	36.9	12.1	10.6	10.2	10.8	12.3
OH^+6	1.848	−33.9	−45.7	11.6	10.1	9.7	10.2	13.0
				Transition State for P−C Bond Cleavage				
TS(P−C)	2.399	−8.4	−179.6	14.4	11.7	9.3	11.0	15.7

[a] Results are presented for the 6-31G(d,p) basis set if not indicated otherwise. [b] Adopted as the ground state. [c] Calculations in 311++G(d,p) basis set.

SCHEME 2: Reaction Pathway of P−C Cleavage; the First Mechanism

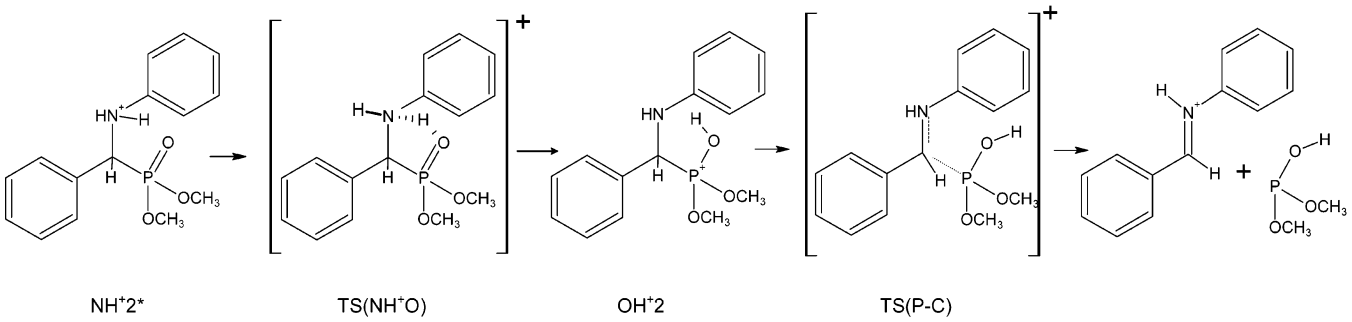

SCHEME 3: Reaction Pathway of P−C Cleavage; the Second Mechanism

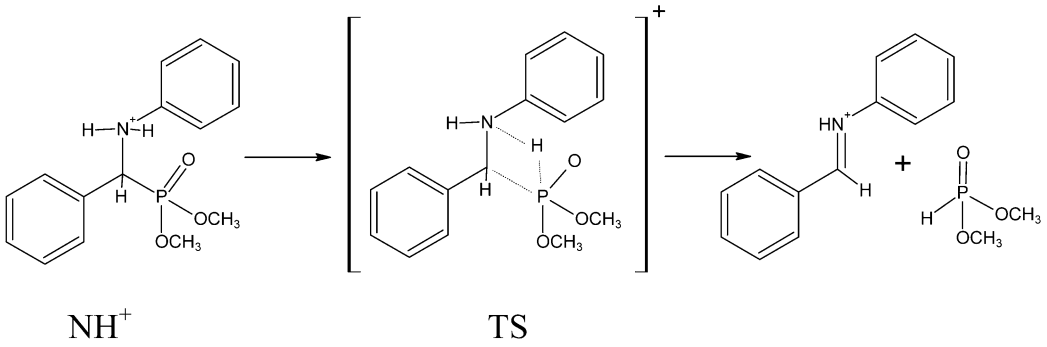

SCHEME 4: Reaction Pathway of P−C Cleavage; the Third Mechanism

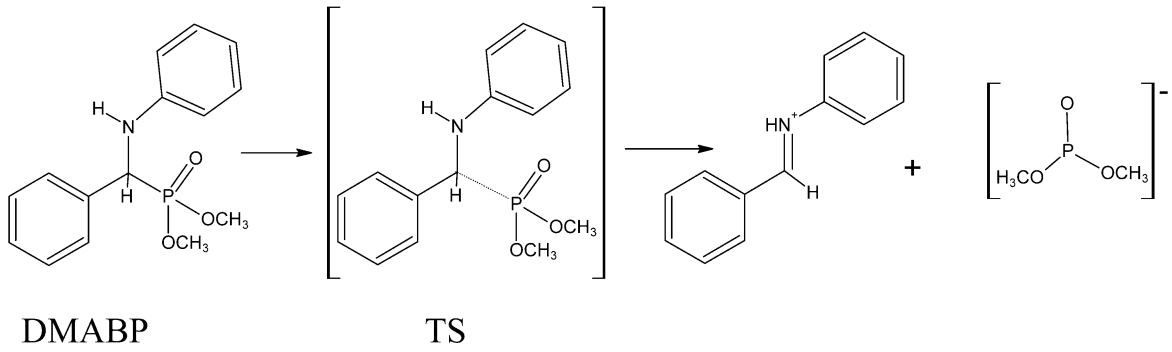

the conformers are stabilized by N−H···O(P) hydrogen bonds. As indicated by their energy differences, the N-protonated conformers (represented as NH^+i ($i = 1-6$), Table 1) have a similar energy trend with respect to the conformers of non-protonated DMABP in the gas phase. In aqueous medium, the energy differences between these conformers are reduced because of the high dipole moment of these protonated species, and the conformer NH^+6 becomes the lowest energy conformer. The corresponding O-protonated conformers (which could be considered as the isomers of N-protonated structures and represented as OH^+i, $i = 1-6$) are higher in energy (by at least 7 kcal/mol) than the N-protonated forms (Table 1). These results thus confirm the preferential protonation of the anilino N atom. In a qualitative sense, this N site is highly basic (a tertiary amine) and thus more easy to protonation than any other site of DMABP. As could be seen from Table 1, these results do not change at higher basis set (6-311++G(d,p)). It validates the use of a smaller basis set in further calculations. The figures representing the structures of the conformers of DMABP and its protonated forms may be found in Supporting Information (Figure 2s−4s).

3.2. Mechanism of the P−C Bond Cleavage. Three different reaction paths could be suggested for the P−C bond cleavage of DMABP in acidic conditions (Schemes 2−4). All of them were suggested before using the available experimental evidence.[14,15,26] The first mechanism (Scheme 2) is the decomposition of the P−C bond due to the protonation of oxygen. While the second probable mechanism (Scheme 3) involves hydrogen transfer from protonated anilino-nitrogen to the phosphorus atom, the third one (Scheme 4) assumes the cleavage of the neutral molecule into cations. The homolytic cleavage leading to two radicals has not been investigated because of the lack of experimental evidence.

TABLE 2: Atomic Charges from the Gross Mulliken Population Analysis for the Atoms of the Reactants, TS, and Products Involved in the Reaction Following the First Mechanism (Charges Are in Electrons)

complex[a]	O	P	C	N	H[b]
NH^+	−0.575	1.151	−0.284	−0.548	0.358
TS(NH^+O)	−0.596	1.254	−0.246	−0.635	0.386
OH^+	−0.498	1.262	−0.230	−0.664	0.377
TS(P−C)	−0.485	1.108	−0.128	−0.617	0.393

[a] See Scheme 2 for the definition of the various complexes. [b] Hydrogen from NH^+···O(P) hydrogen bond.

3.2.1. First Mechanism. As it has been discussed in section 3.1, the protonation of the anilino-N is the first step of this mechanism (Scheme 2) because of its preference over the O-protonation. Since this protonated form is stabilized through

TABLE 3: Structural Parameters for the Reactants, Transition States (TS) and Products for the First Mechanism of the P−C Bond Cleavage Including Two Water Molecules (Represented by W)

complex	l_{N-H}[b]	l_{H-O}[b]	l_{P-C}[b]	α(N−H−O)[c]	τ_1(N−C−P−O)[c]	τ_2(C1−N−C3−C2)[c]
NH^+-WW[a]	1.030	2.206	1.857	119.0	−32.8	−155.9
TS(NH^+O)-WW	1.463	1.124	1.867	145.4	−9.7	−123.0
OH^+-WW[a]	1.864	1.001	1.867	132.8	−18.7	−129.3
TS(P−C)-WW	2.928	0.977	2.234	100.0	13.6	−172.2
product-WW	4.674	0.969	4.500	123.0	34.6	179.7

[a] According to our convention, NH^+ represents N-protonated structure and OH^+ represents O-protonated structure. [b] *l* represents bond lengths (Å). [c] α and τ respectively represents bond angle and torsion angles (degrees).

hydrogen bond formation with the O atom (attached to P), it initiates a proton-transfer mechanism to the O atom. By considering the lowest energy conformer among the N-protonated and O-protonated conformers, a transition state has been located through DFT/B3LYP/QST2/6-31G(d,p) level calculations. This transition state is similar for the cases when all other low-energy N-protonated conformers are considered, and it is characterized by the following parameters: R(N−H) = 1.442 Å, R(O−H) = 1.133 Å, α(N−H−O) = 145.5°, $\tau_1 = -11.8°$, and the free energy of activation of 5.56 kcal/mol (Figure 5s, Supporting Information). The calculation in aqueous medium indicates that water stabilizes the N-protonated structure and it leads to higher free energy of activation (10.24 kcal/mol, Table 1).

The transfer of the proton from nitrogen to the oxygen atom is followed by the P−C bond cleavage. The energetically lowest transition state for decomposition reaction is characterized by the relative energy of 7.47 kcal/mol (in solution) indicating the high probability of such process. Other transition states were also located. However, they are significantly higher in energy. The validity of this transition states was confirmed by the intrinsic reaction coordinate (IRC) analysis.[28] The potential energy profile of this IRC path is given in Supporting Information (Figure 6s).

Five atoms are directly involved in the two-step mechanism of the P−C bond cleavage. The diester fragment (−P(O)-$(OCH_3)_2$) in the nitrogen-protonated complex maintains a large portion of cationic charge of 0.657 *e* as calculated through the gross Mulliken population analysis. The transfer of proton to phosphoryl oxygen leads to an increase of the total cationic charge on diester fragment (0.894 *e*). However, subtracting the charge localized on transferred hydrogen leads to a total charge of 0.517 *e* on the rest of the fragment. The small decrease of excess electron on carbon atom indicates charge polarization of the P−C bond from carbon to phosphorus. The formation of the transition state further polarizes the P−C bond. The transition state with a charge of only 0.457 *e* on the protonated −P(OH)-$(OCH_3)_2$ fragment is suitable for the bond cleavage. The close inspection of atomic charges indicates the significant delocalization of electronic density and the stabilization of protonated imine fragment by phenyl groups. The gross Mulliken population charges presented in Table 2 indicate the modest changes on separate atoms due to structural transformations, which are in agreement with expected electron delocalization.

The influence of the solvent was further investigated by the direct inclusion of two water molecules in this model. The optimized locations of the water molecules were found in the vicinity of the C−N structural fragment. These water molecules form hydrogen bonds along N−H and (P)C−H bonds. The figure presenting structures is included in Supporting Information (Figure 7s). The interactions of water lead to the planar structure of the imine cation, the O-proton transferred product of reaction (Scheme 2). The presence of protonated imine in the reaction environment and its planar geometry in the solution were revealed by NMR studies.[29] Structural parameters of the complexes formed along the reaction path are presented in Table 3. The corresponding thermodynamic characteristics determined using DFT/B3LYP/COSMO model (Table 1) and by explicit representation through hydration by two water molecules (Table 4) are in the close agreement indicating the validity of the solvent model predictions. Both of the approaches predict an increase of the activation free energy due to interaction with the water, which is a crucial test to verify the solvent models. A single water molecule is not sufficient to reproduce the effect of the aqueous solvation. Three molecules, however, do not change the overall picture of the dissociation process, and we concluded that the vital part of the direct hydrogen bonding is revealed by interaction with just two water molecules.

TABLE 4: Energy Differences (kcal/mol) Between the Reactants Transition States and the Products of the P−C Bond Cleavage Including Two Water Molecules for the Reaction Path Involving the First Mechanism (Electronic Energy, Δ*E*; Electronic Energy Corrected for Zero Point Energy, Δ(*E* + ZPE); Free Energy at 293 K, Δ*G*; and Free Energy Including Solvent Effects, ΔG_{aq}) Where Calculated Results Are for 6-31G(d,p) Basis Set if not Indicated Otherwise

complex[a]	Δ*E*	Δ(*E* + ZPE)	Δ(*E* + ZPE)[b]	Δ*G*	ΔG_{aq}
NH^+-WW	0.0	0.0	0.0	0.0	0.0
TS(NH^+O)-WW	13.1	9.6	10.1	9.2	12.2
OH^+-WW	12.5	10.5	10.0	9.8	11.9
TS(P−C)-WW	15.5	13.5	12.0	13.5	16.2
Product -WW	2.8	1.1	−1.0	−0.9	1.3

[a] See Scheme 2 for the definition of the various molecular systems. [b] Calculations in 311++G(d,p) basis set.

Probable transition states, which involves simultaneous protonation and P−C cleavage, were also investigated. However, the optimizations always yielded transition states or reactants of the two-step reaction. Additional studies including protonated DMABP and three water molecules were carried out to investigate the possibility of simultaneous P−C bond cleavage and hydrolysis of imine intermediate. The optimization always located the same transition state as that for the P−C cleavage, or it led to the hydrolysis of the imine product. Again, it supports this two-step reaction, bond decomposition followed by the hydrolysis of imine cation.

3.2.2. Second Mechanism. The proposed mechanism assumes a direct proton transfer from amino group to the phosphorus atom, which leads to H-phosphonate (Scheme 3) through direct decomposition of the P−C bond. The nature of the transition state for the proton transfer from the anilino nitrogen to the O atom (attached to P) is similar to the one revealed by the first mechanism (section 3.2.1). The calculated transition state for the P−C cleavage (Figure 5s, Supporting Information) has a very high free energy of activation (74.1 kcal/mol in the gas phase and 77.3 kcal/mol in aqueous medium), and its validity was confirmed by IRC calculations. The reaction is thus quite unlikely to proceed through this channel. The C−N−H angle

characterizing the transition state is very small and this unfavorable geometric condition causes a very high activation barrier.

3.2.3. Third Mechanism. In this scheme, the neutral DMABP molecule breaks up into ions (Scheme 4). The resulting imine cation is further hydrolyzed, while the anion yielded because the reaction with H_3O^+ forms H-phosphonate. The activation free energy for the transition state amounts to 31.4 kcal/mol (25.4 kcal/mol due to aqueous solvation). The free energy difference between energy barriers of the first and present mechanisms is about 10 kcal/mol. This suggests that the first mechanism is much more probable.

3.2.4. Nature of the Products Yielded from the Final Transition State. The products yielded from the transition states in all of the investigated reaction paths include protonated imine. So its hydrolysis does not influence the course of these reactions. The cleavage of P−C bond, according to the first mechanism, leads to energetically higher tautomeric form of H-phosphonate. H-phosphonate reacting with H_3O^+ and H_2O, through the chain of equilibrium reactions, is converted to its stable form. The free energy of tautomerization amounts to −6.5 kcal/mol.

4. Conclusions

The present theoretical investigation revealed the probable mechanisms of the P−C bond cleavage of α-aminophosphonates (using the model molecule DMABP) in acidic medium, which leads to the derivatives of phosphonic acid. Three probable reaction paths have been taken into account and our results confirm a three-step process, which includes protonation, P−C bond cleavage, and final stabilization of the products from the transition state. The most favorable mechanism consists of amino group protonation (of the aniline fragment), proton transfer through hydrogen bond [NH···O(P)], and P−C bond cleavage leading to the protonated imine and derivatives of H-phosphonate. The imine cation is further hydrolyzed. The calculations were carried out in the gas phase (DFT/B3LYP) as well as in aqueous medium (DFT/B3LYP/COSMO). Explicit inclusion of the H_2O molecules indicated that two water molecules are needed to properly represent the solvent effect on the P−C bond cleavage reaction. More importantly, the agreement of the results of hydration with the continuum model approach for aqueous solvation validates the reliability of the use of DFT/B3LYP/COSMO model in the present case.

Acknowledgment. This research was supported in part by Wroclaw University of Technology, Poland and the DoD through ERDC Grant W912MZ-04-2-0002. This work does not necessarily reflect the policy of the government, and no official endorsement should be inferred. We would like to thank the Mississippi Center for Supercomputing Research, Poznan and Wroclaw Supercomputing and Networking Centers, the Interdisciplinary Center for Mathematical and Computational Modeling of Warsaw University, and Academic Computer Centre in Gdansk (CI TASK) for a generous allotment of computer time.

Supporting Information Available: The time dependent NMR plot for the decomposition of dimethyl (α-anilinobenzyl)-phosphonate (DMABP), figures with optimized molecule and its protonated forms, transition states for NH···O(P) and P−C cleavage, IRC plot for the first mechanism, and figure of structures for the reaction pathway with the direct inclusion of two water molecules. This material is available free of charge via the Internet at http://pubs.acs.org.

References and Notes

(1) Phillips, M. A.; Fletterick, R.; Rutter, W. J. *J. Biol. Chem.* **1990**, *265*, 20692.
(2) Tantillo, D. J.; Houk, K. N. *J. Org. Chem.* **1999**, *64*, 3066.
(3) Kafarski, P.; Lejczak, B. *Curr. Med. Chem.: Anti-Cancer Agents* **2001**, *1*, 301.
(4) Andreeva, I.; Efimtseva, E. V.; Padyukova, N.; Kochetkov, S. N.; Mikhailov, S. N.; Dixon, H. B. F.; Karpeisky, M. Y. *Mol. Biol.* **2001**, *35*, 717.
(5) Dellaria, J. F.; Maki, R. G.; Stein, H. H.; Cohen, J.; Whittern, D.; Marsh, K.; Hoffman, D. J.; Plattner, J. J.; Perun, T. J. *J. Med. Chem.* **1990**, *33*, 534.
(6) Walter, M. W. *Nat. Prod. Rep.* **2002**, *19*, 278.
(7) Kukhar, V. P.; Hudson, H. R. *Aminophosphonic and aminophosphinic acids*; Wiley: New York, 2000.
(8) Jackson, P. F.; Cole, D. C.; Slusher, B. S.; Stetz, S. L.; Ross, L. E.; Donzanti, B. A.; Trainor, D. A. *J. Med. Chem.* **1996**, *39*, 619.
(9) Boduszek, B.; Halama, A. *Phosphorus, Sulfur Silicon* **1998**, *143*, 1.
(10) Boduszek, B.; Latajka, R.; Walkowiak, U. *Pol. J. Chem* **2001**, *75*, 63.
(11) Kurt, M. J.; Olmstead, M. M.; Haddadin, M. J. *J. Org. Chem.* **2005**, *70*, 1060.
(12) Lim, M.; Cramer, C. J. *J. Phys. Org. Chem.* **1998**, *11*, 149.
(13) Lipok, J.; Cierpicki, T.; Kafarski, P. *Phosphorus, Sulfur Silicon* **2002**, *177*, 1657.
(14) Deron, A.; Gancarz, R.; Gancarz, I.; Halama, A.; Kuźma, Ł.; Rychlewski, T.; Zoń, J. *Phosphorus, Sulfur Silicon* **1999**, *437*, 144.
(15) Goldeman, W.; Olszewski, T. K.; Boduszek, B.; Sawka-Dobrowolska, W. *Tetrahedron* **2006**, *62*, 4506.
(16) Parr, R. G.; Yang, W. *Density-Functional Theory of Atoms and Molecules*; Oxford University Press: New York, 1994.
(17) Becke, D. *J. Chem. Phys.* **1993**, *98*, 5648.
(18) Vosko, S. H.; Wilk, L.; Nusiar, M. *Can. J. Phys.* **1980**, *58*, 1200.
(19) Lee, C.; Yang, W.; Parr, R. G. *Phys. Rev. B* **1988**, *37*, 785.
(20) Francl, M. M.; Pietro, W. J.; Hehre, W. J.; Binkley, J. S.; Gordon, M. S.; DeFrees, D. J.; Pople, J. A. *J. Chem. Phys.* **1982**, *77*, 3654.
(21) Krishnan, R.; Binkley, J. S.; Seeger, R.; Pople, J. A. *J. Chem. Phys.* **1980**, *72*, 650.
(22) Peng, C.; Schlegel, H. B. *Israel J. Chem.* **1993**, *33*, 449.
(23) Cossi, M.; Rega, N.; Scalmani, G.; Barone, V. *J. Comput. Chem.* **2003**, *24*, 669.
(24) Davidson, N. *Statistical Mechanics;* McGraw-Hill: New York, 1962.
(25) Frisch, M. J.; Trucks, G. W.; Schlegel, H. B.; Scuseria, G. E.; Robb, M. A.; Cheeseman, J. R.; Montgomery, J. A., Jr.; Vreven, T.; Kudin, K. N.; Burant, J. C.; Millam, J. M.; Iyengar, S. S.; Tomasi, J.; Barone, V.; Mennucci, B.; Cossi, M.; Scalmani, G.; Rega, N.; Petersson, G. A.; Nakatsuji, H.; Hada, M.; Ehara, M.; Toyota, K.; Fukuda, R.; Hasegawa, J.; Ishida, M.; Nakajima, T.; Honda, Y.; Kitao, O.; Nakai, H.; Klene, M.; Li, X.; Knox, J. E.; Hratchian, H. P.; Cross, J. B.; Bakken, V.; Adamo, C.; Jaramillo, J.; Gomperts, R.; Stratmann, R. E.; Yazyev, O.; Austin, A. J.; Cammi, R.; Pomelli, C.; Ochterski, J. W.; Ayala, P. Y.; Morokuma, K.; Voth, G. A.; Salvador, P.; Dannenberg, J. J.; Zakrzewski, V. G.; Dapprich, S.; Daniels, A. D.; Strain, M. C.; Farkas, O.; Malick, D. K.; Rabuck, A. D.; Raghavachari, K.; Foresman, J. B.; Ortiz, J. V.; Cui, Q.; Baboul, A. G.; Clifford, S.; Cioslowski, J.; Stefanov, B. B.; Liu, G.; Liashenko, A.; Piskorz, P.; Komaromi, I.; Martin, R. L.; Fox, D. J.; Keith, T.; Al-Laham, M. A.; Peng, C. Y.; Nanayakkara, A.; Challacombe, M.; Gill, P. M. W.; Johnson, B.; Chen, W.; Wong, M. W.; Gonzalez, C.; Pople, J. A. *Gaussian 03*, revision C.02; Gaussian, Inc.: Wallingford, CT, 2004.
(26) Ruzic-Torus, Z.; Tusek-Bozic, L. *Acta Crystallogr., Sect. C* **2004**, *60*, 434.
(27) Doak, G. O.; Freedman, L. D. *Chem. Rev.* **1960**, *61*, 31.
(28) Schlegel, H. B. In *Modern Electronic Structure Theory*; Yarkony, D. R., Ed.; World Scientific: Singapore, 1994.
(29) Xu, H.; Sohlberg, K.; Wei, Y. *J. Mol. Struct.* **2003**, *634*, 311.